

# Wide-Range Automated Wavelength Calibration Over a Full FSR in a Dual-Ring based Silicon Photonic Switch

Qingming Zhu<sup>1</sup>, Hongxia Zhang<sup>1</sup>, Ruiyuan Cao<sup>1</sup>, Ning Zhao<sup>1</sup>, Xinhong Jiang<sup>1</sup>, Danping Li<sup>2</sup>, Yanbo Li<sup>2</sup>, Xiaolu Song<sup>2</sup>, Xuhan Guo<sup>1</sup>, Yong Zhang<sup>1</sup>, and Ciyuan Qiu<sup>1</sup>

<sup>1</sup>State Key Laboratory of Advanced Optical Communication Systems and Networks,

Department of Electronic Engineering, Shanghai Jiao Tong University, Shanghai 200240, China

<sup>2</sup>Network Research Department, Huawei Technologies Co., Ltd., Shenzhen 518129, China

Author e-mail address: [qiuciyuan@sjtu.edu.cn](mailto:qiuciyuan@sjtu.edu.cn)

**Abstract:** We demonstrate an automated wavelength calibration scheme for a dual-ring based silicon electro-optic switch. By using an improved saddle point searching algorithm, the calibration over a full free spectral range of 6 nm is achieved.

**OCIS codes:** (130.3120) Integrated optics devices; (130.4815) Optical switching devices; (230.4555) Coupled resonators.

## 1. Introduction

To address the power consumption and latency issues in large-scale switching applications, optical switching has become a promising candidate [1]. In general, a wavelength division multiplexed (WDM) switching network consists of multiple single-wavelength switching layers [2]. Based on this architecture, some optical switching schemes have been proposed by using various device structures [3]. Among these schemes, resonator-based devices are attractive because of low power consumptions and compact footprints [4]. Optical switches based on high-order resonators can construct desired spectral characteristics such as flat-top and sharp-edge responses [5]. However, wavelength calibration of such devices is challenging, as the resonance wavelengths are sensitive to fabrication and temperature variations. Automated calibration schemes for high-order micro-ring based filters have been previously proposed based on maximum searching [5,6] and saddle point searching (SPS) [7] algorithms. However, these calibration schemes were only demonstrated for a single operation wavelength with the TO tuning ranges of 0.1 free spectral range (FSR) [5], 0.2 FSR [6] and 0.3 FSR [7], respectively. To date, automated wavelength calibration of high-order resonator based switches with a full-FSR tuning range has not been reported.

In this paper, for the first time to the best of our knowledge, automated wavelength calibration over a full FSR is experimentally demonstrated in an O-band dual-ring resonator based  $2 \times 2$  silicon photonic switch. The switch unit consists of two closely coupled ring resonators, micro-heaters, and Ge photodiodes. To achieve the large calibration range, an improved SPS algorithm is proposed based on [7] but with a different searching method, enabling effective mitigation of the thermal crosstalk effects during the TO tuning process. The control algorithm is employed in an off-chip control sub-system to realize the automated wavelength calibration for a fabricated O-band  $2 \times 2$  silicon electro-optic (EO) switch.

## 2. Device structure and sub-system configurations

Fig. 1(a) shows a general control sub-system configuration for the dual-ring resonator based  $2 \times 2$  switch. In the switch, two ring resonators are coupled with each other, and each ring resonator is integrated with a micro-heater, a p-i-n diode and a Ge photodiode along with a power monitoring port. After on-chip optical-to-electrical conversion, the monitored electrical signals from the photodiodes are amplified by trans-impedance amplifiers (TIAs) and then sampled by analog-to-digital converters (ADCs). An automated wavelength calibration algorithm implemented in a centralized processor calculates the TO tuning powers based on the monitored signals, thus forming a feedback control. After calibrating the resonance wavelengths of both resonators, fast switching can be subsequently realized

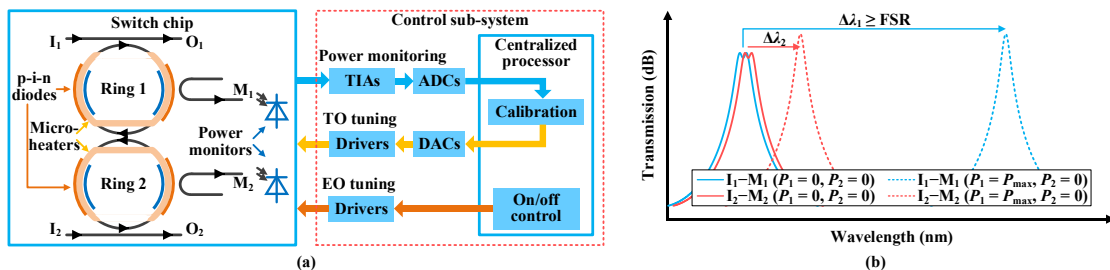


Fig. 1. (a) Schematic diagram of the  $2 \times 2$  switch and the control sub-system. TIAs: trans-impedance amplifiers, ADCs: analog-to-digital converters, DACs: digital-to-analog converters. (b) Illustration of the thermal crosstalk effects during the TO tuning process.  $P_i$  ( $i = 1, 2$ ) is the TO tuning power applied to Ring  $i$ .  $P_{\max}$  is the maximal tuning power.

by the processor-controlled EO tuning signals. Note that this sub-system configuration can be applied to a general  $N \times N$  switching network with a similar scheme as in [7].

In the wavelength calibration process, the main challenge is the thermal crosstalk between the two closely coupled ring resonators. As illustrated in Fig. 1(b), the TO tuning power  $P_1$  applied to Ring 1 should be large enough to achieve the full-FSR tuning range  $\Delta\lambda_1$ , however the induced thermal crosstalk causes a significant resonance wavelength detuning  $\Delta\lambda_2$  of Ring 2 during the calibration process, and vice versa. The value of  $\Delta\lambda_2$  can be calculated according to the thermal isolation function of the device [8].

### 3. Operation principle and algorithm design

The aforementioned thermal crosstalk effects limit the calibration range in [7], which will be illustrated in the following discussion. The monitored power output of  $M_1$  is denoted by  $P_M$  if the optical power fed into  $I_1$  is larger than that fed into  $I_2$ , and vice versa.  $\phi_1$  and  $\phi_2$  represent the round-trip phases of Ring 1 and Ring 2, respectively. It is analyzed in [7] that  $P_M(\phi_1, \phi_2)$  follows a saddle shape with proper structural parameters. A SPS algorithm consisting of several sub-processes is then developed to find the saddle point where  $\phi_1 = \phi_2 = 0$ . The local maximum/minimum of  $P_M$  during each sub-process is denoted as  $P_{M\_max}/P_{M\_min}$ . In the first sub-process, only  $\phi_1$  is tuned to search for  $P_{M\_max}$ . In the second sub-process, only  $\phi_2$  is tuned to search for  $P_{M\_min}$ . Then the two sub-processes are carried out for two iterations to finely tune  $\phi_1$  and  $\phi_2$ . However, if the initial round-trip phases are relatively large, the large TO tuning power in the second sub-process causes significant detuning of  $\phi_1$ . Therefore, such an algorithm can achieve only a small calibration range.

Based on the work in [7], we propose an improved SPS algorithm consisting of four sub-processes (i)–(iv) to mitigate the thermal crosstalk effects in the dual-ring resonator based switch. In sub-process (i),  $\phi_1$  and  $\phi_2$  are simultaneously tuned to search for  $P_{M\_max}$ . Since the initial phase difference between  $\phi_1$  and  $\phi_2$  due to fabrication variations is small relative to the full tuning range of  $2\pi$ , this leads to  $\phi_1 \approx \phi_2 \approx 0$  after sub-process (i). Thus, the following sub-processes can be fine tuning processes and experience weak thermal crosstalk. The pseudo-code and phase calibration effects of the improved SPS algorithm are shown in Fig. 2(a) and (b), respectively.

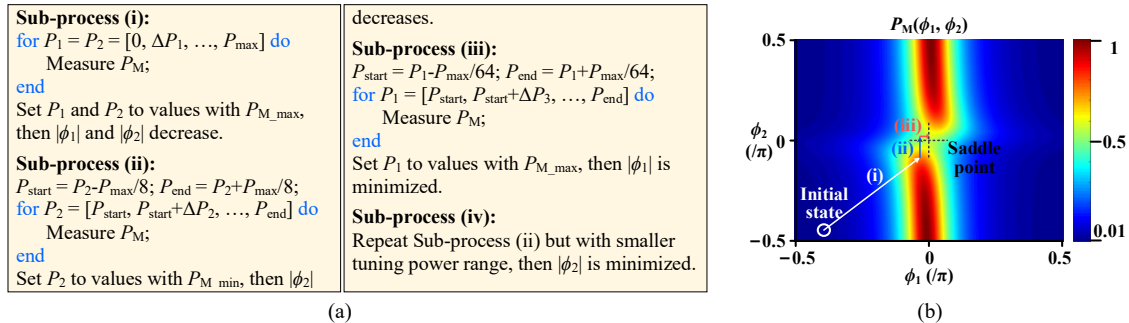


Fig. 2. Improved SPS algorithm. (a) Pseudo-code. (b) Illustration of the phase calibration effects.

### 4. Device design, fabrication and experimental results

The schematic of the  $2 \times 2$  switch is shown in Fig. 3(a). In the switch design, the radii of the two coupled ring resonators are  $10 \mu\text{m}$  and the coupling gap between them is  $400 \text{ nm}$ . The gap between each ring resonator and the straight waveguide is  $240 \text{ nm}$ . In each ring resonator, a  $\sim 98:2$  directional coupler is integrated as a power monitoring port. This  $2 \times 2$  switch was fabricated by a shuttle run in IME Singapore. The footprint of the switch unit is  $934 \mu\text{m} \times 615 \mu\text{m}$ . A vertical coupling system is used to couple light into and out of the device. The coupling loss is measured to be  $\sim 5 \text{ dB/facet}$ . The device is wire-bonded to interface with the circuits.

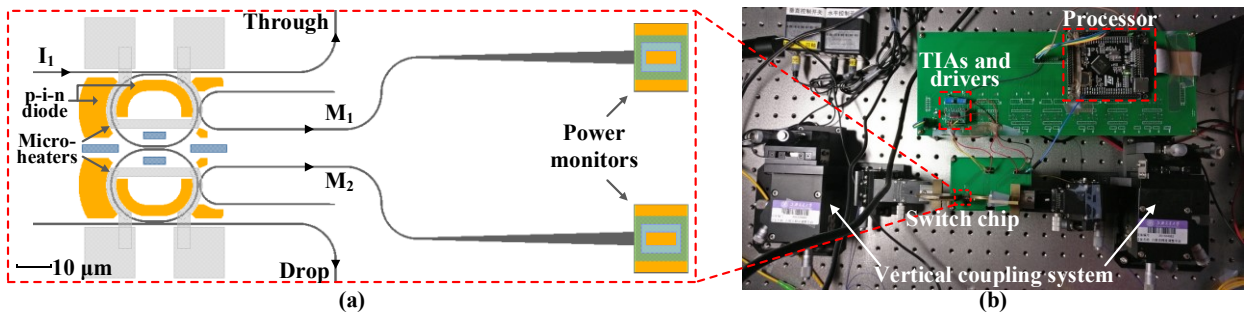


Fig. 3. (a) Schematic of the  $2 \times 2$  switch. (b) Photograph of the experimental setup.

The photograph of the control sub-system and the controlled switch fabric is provided in Fig. 3(b). In the sub-system, two TIAs following the on-chip Ge photodiodes are designed with  $\sim 10^5$ -V/A gains and  $\sim 20$ -KHz bandwidths. The ADCs and DACs are integrated in a single-core processor (STM32F407VET6), with the same resolution of 12 bits and  $< 5$ - $\mu$ s conversion times. The calibration algorithm and a switching on/off operation are also implemented in the processor, and the thermal feedback control period of the sub-system is  $\sim 50$   $\mu$ s, which is dominated by the TO response times of the device.

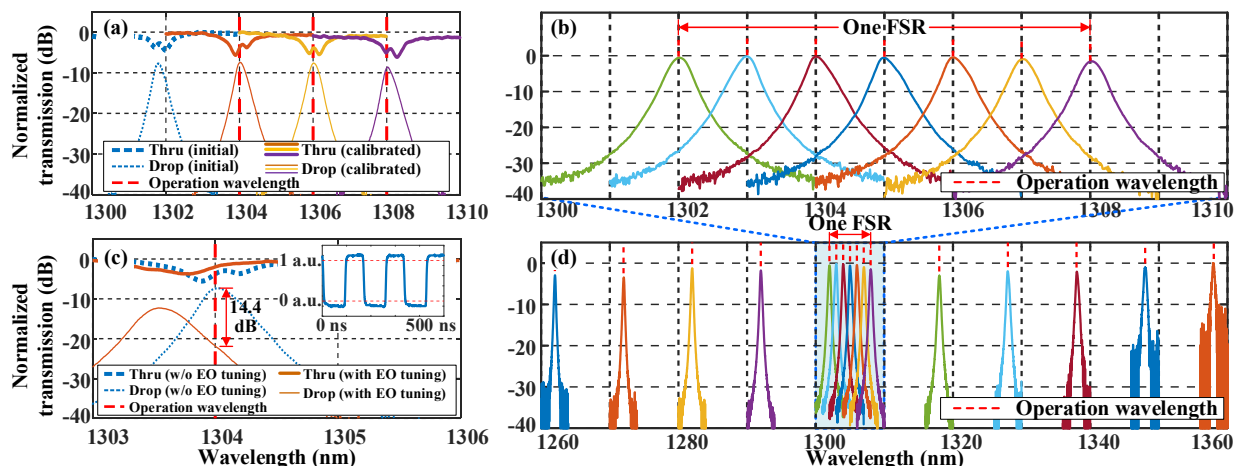


Fig. 4. Normalized transmission spectra (a) with and without the calibration. (b) with the operation wavelength varying within the full FSR. (c) with and without the EO tuning. (d) with the operation wavelength varying within the full O band.

The wavelength calibration scheme is experimentally demonstrated. Firstly, the normalized transmission spectra at the two output ports with and without the calibration are shown in Fig. 4(a). For each of three operation wavelengths, the resonance wavelengths of the two calibrated ring resonators are red-shifted to the operation wavelength. Then, we measured the transmission spectra at the drop port with the operation wavelength varying in a 1-nm step over the full FSR of 6 nm, and similarly in a 10-nm step over the full O band, which are normalized and provided in Fig. 4(b) and (d), respectively. The calibration over O band is based on the periodic spectrum of the dual-ring resonator. For all these spectra, the insertion losses at the operation wavelength vary within a 3.5-dB range. The average duration of the calibration processes is  $\sim 4$  ms and the TO tuning power to achieve the 6-nm tuning range is  $\sim 210$  mW. Note that although a single optical input is used in the measurements, the SPS algorithm also applies to the dual-input case [7]. Finally, fast switching is realized by using the EO tuning. As depicted in Fig. 4(c), by applying an EO tuning power of 12 mW, the resonance wavelengths are detuned by 0.5 nm, thus achieving 14.4 dB extinction ratio at the drop port. The inset shows the waveform of the EO response, where the 10%–90% switching times for the rise edge and the fall edge are 5.5 ns and 6.9 ns, respectively.

## 5. Conclusion

We experimentally demonstrate an automated wavelength calibration scheme based on an improved SPS algorithm for an O-band  $2 \times 2$  silicon EO switch using a dual-ring resonator. By mitigating the thermal crosstalk effects, the calibration algorithm can now operate over a full FSR of 6 nm.

## 6. Reference

- [1] R. G. Beausoleil, P. J. Kuekes, G. S. Snider, S. Y. Wang, and R. S. Williams, "Nanoelectronic and nanophotonic interconnect," *Proc. IEEE* **96**, 230-247 (2008).
- [2] Y. J. Xiong, M. Vandenhouste, and H. C. Cankaya, "Control architecture in optical burst-switched WDM networks," *IEEE J. Sel. Areas Commun.* **18**, 1838-1851 (2000).
- [3] Y. Li, Y. Zhang, L. Zhang, and A. W. Poon, "Silicon and hybrid silicon photonic devices for intra-datacenter applications: state of the art and perspectives," *Photon. Res.* **3**, B10-B27 (2015).
- [4] A. Deore, O. Turku, S. Ahuja, S. J. Hand, and S. Melle, "Total cost of ownership of WDM and switching architectures for next-generation 100Gb/s networks," *IEEE Commun. Mag.* **50**, 179-187 (2012).
- [5] H. Jayatilaka, K. Murray, M. A. Guillen-Torres, M. Caverley, R. Hu, N. A. F. Jaeger, L. Chrostowski, and S. Shekhar, "Wavelength tuning and stabilization of microring-based filters using silicon in-resonator photoconductive heaters," *Opt. Express* **23**, 25084-25097 (2015).
- [6] J. C. C. Mak, W. D. Sacher, J. C. Mikkelsen, T. Y. Xue, Z. Yong, and J. K. S. Poon, "Automated calibration of high-order microring filters," in *Conf. on Lasers and Electro-Optics*, 2015, Paper SWIN.2.
- [7] Q. Zhu, X. Jiang, Y. Yu, R. Cao, H. Zhang, D. Li, Y. Li, L. Zeng, Y. Zhang, X. Guo, and C. Qiu, "Automated wavelength alignment in a  $4 \times 4$  silicon thermo-optic switch based on dual-ring resonators," *Submitted to IEEE Photon. J.*, (2017).
- [8] T. Wipiejewski, D. B. Young, B. J. Thibeault, and L. A. Coldren, "Thermal crosstalk in  $4 \times 4$  vertical-cavity surface-emitting laser arrays," *IEEE Photon. Technol. Lett.* **8**, 980-982 (1996).